

**An Unprecedented-Type Intramolecular Redox Reaction of Solid Tetraamminecopper(2+) Bis(permanganate) ( $[\text{Cu}(\text{NH}_3)_4](\text{MnO}_4)_2$ ) – A Low-Temperature Synthesis of Copper Dimanganese Tetraoxide-Type ( $\text{CuMn}_2\text{O}_4$ ) Nanocrystalline Catalyst Precursors**

by László Kótai<sup>a\*</sup>), Kalyan K. Banerji<sup>b)</sup>), István Sajó<sup>a)</sup>), János Kristóf<sup>c)</sup>), B. Sreedhar<sup>d)</sup>), Sándor Holly<sup>a)</sup>), Gábor Keresztury<sup>a)</sup>), and Antal Rockenbauer<sup>a)</sup>

<sup>a)</sup> Chemical Research Center, Hungarian Academy of Sciences, Pusztaszeri u. 59–67, H-1025 Budapest (e-mail: kotail@chemres.hu)

<sup>b)</sup> Department of Chemistry, J. N. V. University, Jodhpur, 342005, Jodhpur, India

<sup>c)</sup> University of Veszprém, Egyetem u. 10, H-8200, Veszprém

<sup>d)</sup> Inorganic Chemistry Division, Indian Institute of Chemical Technology, Hyderabad 500007, India

---

Tetraamminecopper(2+) bis(permanganate) ( $[\text{Cu}(\text{NH}_3)_4](\text{MnO}_4)_2$ ; **1**) was prepared, and its properties were studied in both aqueous solution and the solid phase. The presence of H-bond interactions between the ammonia ligand of the complex cation and an O-atom of the permanganate ion was detected by IR and Raman methods. The solid-phase thermal deammoniation of **1** led to an unusual intramolecular redox reaction between the Mn–O...H–N linkage with formation of  $\text{NH}_4\text{NO}_3$  and  $\text{CuMn}_2\text{O}_4$ -type mixed oxides instead of stepwise deammoniation, even below 100°. The thermal deammoniation of **1** in aqueous solution led, instead of to hydrated copper(2+) bis(permanganate), to the formation of  $\text{NH}_4\text{MnO}_4$  (**2**). Since the temperature of the thermal deammoniation of **1** is lower than the decomposition temperature of the permanganate ion, the regulated solid-phase decomposition of **1** allowed preparation of  $\text{CuMn}_2\text{O}_4$ -type oxides with mixing of copper and manganese at the atomic level.

---

**Introduction.** – Solid-state precursors with copper and manganese ions (mixed at the atomic level) can be useful for the synthesis of various catalysts [1] at moderate temperatures. One of the possible precursors, tetraamminecopper(2+) bis(permanganate) ( $[\text{Cu}(\text{NH}_3)_4](\text{MnO}_4)_2$ ; **1**), was discovered by Klobb [2]. Müller *et al.* [3] studied its IR spectrum and determined its powder diffractogram, but this diffractogram could not be indexed due to the presence of an unidentified contaminant. Gorbunov and Shmagin [4] compared the ignition properties of **1** with other tetraamminecopper(2+) salts. An unidentified contaminant was also found in their samples. Seferiadis *et al.* [5] reported the results of thermal studies and single-crystal structure determination of **1** and concluded that strong H-bonds are lacking in **1**. The authors assumed stepwise deammoniation and decomposition of **1**, with formation of  $\text{CuMn}_2\text{O}_4$ -type catalyst precursors *via* a  $\text{Cu}(\text{MnO}_4)_2$  intermediate at around 500 K. However, no explanation has been offered for the unusual chemical and thermal properties of **1**. Also, the nature of the contaminant has not yet been exactly described.

To clarify the nature of the contaminant, we performed some new studies on the behavior of **1** in solution. We identified this contaminant as ammonium permanganate ( $\text{NH}_4\text{MnO}_4$ ; **2**) [6]. Since the presence of **2** may cause some overlap of N–H or Mn–O bands, the IR data of **1** were re-investigated, and some studies were made

by Raman, ESR, and TG-MS (TG = thermogravimetry) as well as by powder X-ray-diffraction methods. The decomposition product of **1** was studied by IR, MS, and powder X-ray diffraction. Based on our thermal investigations, we suggest the occurrence of an unprecedented intramolecular redox reaction in solid **1**, which offers a new possibility for the preparation of  $\text{CuMn}_2\text{O}_4$ -type catalyst precursors at low temperature. We give a possible explanation for the unusual chemical and thermal properties of **1** related to the presence of a weak H-bonding interaction within this compound.

**Experimental.** – *General.* Freshly prepared pure materials were used with the exception of some DSC (differential scanning calorimetry) studies in which the effect of the contaminating  $\text{NH}_4\text{MnO}_4$  (**2**; eventually formed on aging of wet **1**) on the thermal properties of ( $[\text{Cu}(\text{NH}_3)_4](\text{MnO}_4)_2$ ; **1**) was investigated. Solid-state IR spectra: *BioRad-Digilab FTS-45-FT-IR* spectrometer for the  $4000\text{--}400\text{ cm}^{-1}$ , and *BioRad-Digilab FTS-40-FIR* spectrometer for the  $400\text{--}40\text{ cm}^{-1}$  range (in nujol mull); **1** decomposed under the conditions of KBr pellet preparation (pressure); to prevent decomposition of the sample, diffuse-reflectance investigations with a *Nicolet 170SX-FT-IR* spectrometer (5% **1** in KBr;  $400\text{--}4000\text{ cm}^{-1}$ ) with  $1\text{ cm}^{-1}$  wavenumber resolution were performed. Solution IR spectra: in DMF; *Nicolet 205-FT-IR* spectrometer for the  $400\text{--}4000\text{ cm}^{-1}$  range. Solid-state Raman spectrum: *Nicolet 950-FT-Raman* spectrometer equipped with a Nd:YAG laser ( $4000\text{--}100\text{ cm}^{-1}$  range,  $1\text{ cm}^{-1}$  resolution); to avoid heating, the sample was rotated during measurements. X-Ray powder diffraction: *Philips PW-1050-Bragg-Brentano* parafocusing goniometer, equipped with secondary-beam graphite monochromator and proportional counter; scans recorded in step mode by using  $\text{CuK}\alpha$  radiation at 40 kV and 35 mA tube power; evaluation of the diffraction patterns by full-profile fitting techniques. Thermal studies: *Derivatograph*-type simultaneous thermoanal. equipment (*Hungarian Optical Works*, Budapest), equipped with a selective  $\text{H}_2\text{O}$  monitor and a gas-titrimetric apparatus ( $\text{NH}_3$  was absorbed and determined by pH-static titration with 0.1M HCl at pH 5); or *Perkin-Elmer DSC-2*-type calorimeter as well as a *Perkin-Elmer TGS-2* thermobalance connected to a *Balzers QMS-511*-type mass spectrometer; heating rates  $5^\circ/\text{min}$  (slow) and  $20^\circ/\text{min}$  (fast); diluted samples (95%  $\text{Al}_2\text{O}_3$  and 5% **1**, covered with  $\text{Al}_2\text{O}_3$ ) under Ar. ESR: *Jeol JES-FE/3X-ESR* spectrometer upgraded for data acquisition by *IBM PC Pentium I*, working in X microwave band with 100 kHz field modulation,  $\text{Mn}^{\text{II}}$ -doped magnesium oxide powder for the calibration of *g*-measurements.

*Tetraamminecopper(2+) Sulfate.*  $\text{CuSO}_4 \cdot 5\text{H}_2\text{O}$  (50 g, 200 mmol) was dissolved in a mixture of  $\text{H}_2\text{O}$  (50 ml) and conc.  $\text{NH}_3$  soln. (80 ml). After 5 min stirring, the soln. was filtered, and MeOH (75 ml) was added to the filtrate. The precipitate was separated and recrystallized from  $\text{H}_2\text{O}$  at  $0^\circ$ . The crystals were subsequently washed with conc.  $\text{NH}_3$  soln. EtOH 1:1, MeOH, and  $\text{Et}_2\text{O}$  and then dried at r.t.: 11.3 g (23.0%) of  $[\text{Cu}(\text{NH}_3)_4]\text{SO}_4 \cdot \text{H}_2\text{O}$ .

*Tetraamminecopper(2+) Bis(permanganate) (1).* A soln. of  $[\text{Cu}(\text{NH}_3)_4]\text{SO}_4 \cdot \text{H}_2\text{O}$  (2.5 g, 10 mmol) in  $\text{H}_2\text{O}$  (15 ml) was cooled to  $+8^\circ$ . Then a 15-ml portion of a cold  $\text{KMnO}_4$  soln. (3.2 g, 20 mmol) was added. The mixture was immediately cooled to  $2^\circ$ : 1.2 g (32%) of **1**. The *d* values of the product and calculated *d* values from single-crystal X-ray data showed a good agreement.

**Results and Discussion.** – *Preparation and Properties.* Preparation of **1** was carried out by the reaction of potassium permanganate and a tetraamminecopper(2+) sulfate solution at  $8^\circ$ , followed by quick cooling of the solution mixture to  $2^\circ$ . Mixing the room-temperature saturated solutions of  $[\text{Cu}(\text{NH}_3)_4]\text{SO}_4$  and  $\text{KMnO}_4$  in a stoichiometric ratio led to the formation a contaminated crystalline mass of **1** in the quenched solution [3][4]. The reaction of the copper(2+) sulfate solution in ammonia containing excess of the latter and  $\text{KMnO}_4$  also gave contaminated **1** at  $8^\circ$  [2], while  $\text{MnO}_2$  formation was observed at room temperature. The purity of **1** decreased with the increase in excess ammonia and increased with the decrease in mixing temperature. Recrystallization of **1** was carried out below  $5^\circ$  [5] to avoid  $\text{NH}_4\text{MnO}_4$  formation [6].

Sample **1** is a violet crystalline substance, soluble in  $\text{H}_2\text{O}$ , DMF, and  $\text{Ac}_2\text{O}$  and insoluble in hydrocarbons and chlorinated solvents. It is stable in dry solid state for

several weeks but decomposes with formation of  $\text{MnO}_2$  if allowed to stand for a longer period of time. The wet crystals of **1** slowly decompose  $> 10^\circ$ . Therefore, the chemical and thermal behavior of **1** strongly depends on the conditions used for drying and the age of the sample due to the presence of decomposition products. Compound **1** also decomposes on standing in solutions, the decomposition product being  $\text{NH}_4\text{MnO}_4$  in  $\text{H}_2\text{O}$ ,  $\text{MnO}_2$  in DMF, and an unidentified green compound in  $\text{Ac}_2\text{O}$ . In DMF solutions, **1** is completely dissociated to its free ions. The permanganate band at  $900\text{ cm}^{-1}$  is a very sharp *s* due to the regular tetrahedral symmetry of the completely solvated  $\text{MnO}_4^-$  ion, and the Cu–N band near  $420\text{ cm}^{-1}$  is broadened due to solvation of the cation *via* the N-atoms of DMF molecules. The DMF solution of **1** loses its purple color within half an hour.

Concentration of the aqueous solution of **1** to half of its initial volume by evaporation leads to the formation of  $\text{NH}_4\text{MnO}_4$  (**2**) due to a quasi-intramolecular acid-base reaction of **1** (both  $\text{Cu}^{2+}$  and  $\text{OH}^-$  ions originate from the dissociation of the tetramminecopper-complex cation) [6] (*Eqn. 1*). An increase in temperature favorably affects the formation of **2**, since the solubility of **1** increases; therefore, the amount of the dissociated tetraamminecopper(2+) ion, as well as the concentrations of the free (released) copper(2+) ions and  $\text{NH}_3$ , also increase. The dissociation of the tetramminecopper(2+) ion to copper(2+) ion and  $\text{NH}_3$ , the protonation of  $\text{NH}_3$ , the formation and dissociation of  $\text{NH}_4\text{OH}$ , as well as the formation of the solubility product of copper(2+) dihydroxide in this system are temperature-dependent processes, thus the reaction according to *Eqn. 1* is also temperature-dependent. Upon bringing the aqueous solution of **1** to the boil, loss of  $\text{NH}_3$  ammonia into the gas-phase shifts the equilibrium to the formation of **2**.



Since contamination of **1** with **2** during room-temperature synthesis or in the presence of excess  $\text{NH}_3$  may be attributed to these processes, the preparation of **1** has to be made at low temperature and in the absence of excess ammonia.

*Structural Characterization.* Compound **1** crystallizes in monoclinic symmetry, with the lattice parameters  $a = 5.413$ ,  $b = 9.093$ ,  $c = 10.749\text{ \AA}$ , and  $\gamma = 96.18^\circ$  at 293 K ( $Z = 2$ ). The central Cu-atom in **1** lies in a near-regular tetragonal plane of an octahedron, and the two axial  $\text{MnO}_4^-$  ions are crystallographically nonequivalent [5]. The ESR *g*-factors ( $g_{zz} = 2.273$ ,  $g_{xx} = g_{yy} = 2.090$ ) are typical of O-ligation with square-planar geometry. The ESR spectrum of **1** has sharp parallel and perpendicular bands. The sharpness of the line and the lack of Cu hyperfine structure show that the exchange interactions between magnetically equivalent Cu-centers are much stronger than the dipole couplings.

Since localization of the H-atoms by X-ray-diffraction measurements is rather uncertain, the possible existence of some H-bonding interactions was investigated by FT-IR and *Raman* methods. Although the position of the  $\tilde{\nu}_{\text{as}}\text{ N-H}$  stretching bands is usually applied for evaluation of the H-bonding ability of the N–H bond, it cannot unambiguously prove the presence of  $\text{N-H}\cdots\text{O}$  H-bonds; however, the shift of the  $\rho_i(\text{NH})$  band in tetraammine metal complexes is very sensitive to the presence of H-bonds [7].

The bands observed in the IR and *Raman* spectra of polycrystalline **1** (see *Fig. 1* and *Table 1*) can roughly be divided into bands originating from the vibrations of the  $\text{MnO}_4^-$  ions, those arising from some modes localized within the  $\text{NH}_3$  molecules in the complex, and those due to the vibrational modes of the complex cation. Although the same number of bands may appear both in the IR and *Raman* spectra of the  $[\text{Cu}(\text{NH}_3)_4]^{2+}$  group ( $C_{4v}$  or  $C_{4h}$  point groups [8];  $C_s$  site symmetry,  $C_{2h}^2$  factor group for compound **1**), we could not assign all the *Raman* shifts of the cation due to their low intensities. To avoid the disturbance of the  $\text{NH}_4\text{MnO}_4$  bands, the IR and *Raman* spectra of **1** were compared to those of **2** [9]. The IR and *Raman* bands of **1** were assigned, based on earlier spectroscopic analyses of the  $[\text{Cu}(\text{NH}_3)_4]^{2+}$  ion and the IR data of square-planar tetraamminecopper(2+) tetraoxometallate complexes [10][11]. The positions of the N–H bands also show structural similarity between **1** and other tetraamminecopper(2+) tetraoxometallates [10][11].

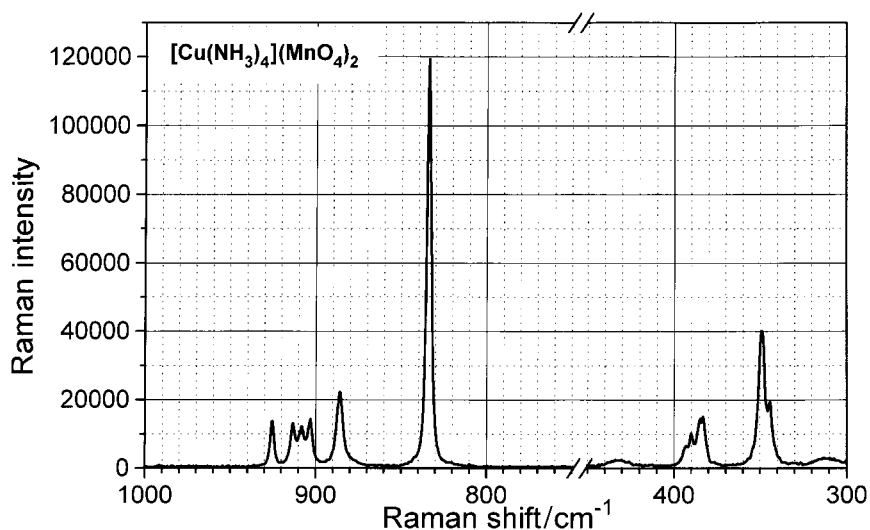


Fig. 1. *Raman* spectrum of **1** at room temperature

The analysis of the Mn–O bands seems to be very interesting due to the distorted structure of **1**. Compound **1** crystallizes in the monoclinic space group ( $C_{2h}^2 - P2_1/m$  with  $Z=2$ ) with two crystallographically nonequivalent  $\text{MnO}_4^-$  ions. The correlation table of  $\text{MnO}_4^-$  ion in **1** is given in *Table 2*.

On the basis of *Table 2*, two  $s$  ( $\tilde{\nu}_1$ ), two  $d$  ( $\tilde{\nu}_2$ ), and two times two  $t$  ( $\tilde{\nu}_3$  or  $\tilde{\nu}_4$ ) bands may be expected in both the *Raman* and IR spectra due to the presence of two crystallographically nonequivalent  $\text{MnO}_4^-$  ions. Since some bands overlap in the spectra recorded at room temperature, the asymmetric Mn–O stretching band ( $\tilde{\nu}_3$ ) in the IR spectra of **1** is a  $d$  or  $q$  (nujol and KBr/diffuse reflectance, resp.), and a well-separated *quint.* can be seen in the *Raman* spectrum. The symmetric Mn–O stretching band ( $\tilde{\nu}_1$ ) is a  $s$  in both spectra, but its intensity in the *Raman* spectrum is higher than in the IR spectrum. Separation of the  $\tilde{\nu}_1$  bands of the two nonequivalent  $\text{MnO}_4^-$  ions cannot be

Table 1. Assignment of IR and Raman Bands of **1**. IR Wavenumbers and Raman shifts are in  $\text{cm}^{-1}$ ; d.r. = diffuse reflectance.

		IR (nujol)	IR (d.r., KBr)	Raman (d.r., KBr)	IR [9] (nujol)
Anion bands:	$\tilde{\nu}_s$ (MnO)	833	833	834	836
	$\tilde{\nu}_{as}$ (MnO)	892	892	886	891
		914	904	903	918
			913	908	
			915	913	
				925	
	$\delta_s$ (OMnO)	345	–	344	–
				349	
	$\delta_{as}$ (OMnO)	392	–	383	–
				385	
390					
			393		
Cation N–H bands:	$\tilde{\nu}_{as}$ (NH)	3328	3325	3323	–
	$\tilde{\nu}_s$ (NH)	3230	3249	3252	–
		3203	3168		
		3167			
	$\delta_{as}$ (HNH)	1620	1604	1592	1615
	$\delta_s$ (HNH)	1240		1270	1244
				1251	
				1239	
			1236		
$\rho_r$ (NH)	675		693	685	
			686		
Cation bands <sup>a</sup> ):	$\tilde{\nu}_{as}$ (CuN)	430	430	431	440
			424		
	$\tilde{\nu}_s$ (CuN)	379	402		–
	$\delta_s$ (NCuN)	305		311	–
	$\gamma$ (CuN <sub>4</sub> )	248			250
	$\pi$ (CuN <sub>4</sub> )	160			
$\tilde{\nu}$ (Cu–O)	194			200	

<sup>a</sup>) Tentative assignment, lattice vibrations were also detected at 118, 89, or 70  $\text{cm}^{-1}$ . IR combination bands were observed at 2444  $\text{cm}^{-1}$ , 1757, 1739, and 1712  $\text{cm}^{-1}$ , 1403  $\text{cm}^{-1}$ , and 624  $\text{cm}^{-1}$ .

Table 2. Correlation Table for Vibrations of Permanganate Ion in **1**

Symmetry of free ion	Site symmetry	Factor group
$T_d$	$C_s$	$C_{2h}^2$ ( $Z=2$ )
$A_1$	$A'$	$A_g + B_u$
$E$	$A'$	$A_g + B_u$
	$A''$	$A_u + B_g$
$2 \times F_2$	$2 \times 2A'$	$2 \times 2(A_g + B_u)$
	$2 \times A''$	$2 \times (A_u + B_g)$

observed. Similar overlaps can be seen in both the  $\delta_s$  and  $\delta_{as}$  (OMnO) deformation bands. The bands at 1739 and 1712  $\text{cm}^{-1}$  are the combination of  $\tilde{\nu}_1$  and  $\tilde{\nu}_3$  modes of the  $\text{MnO}_4^-$  ion (a similar combination band was detected in the diffuse-reflectance IR spectra of both  $\text{NH}_4\text{MnO}_4$  and  $\text{KMnO}_4$  [9]). A  $d$  ( $\delta_s$ ) and a  $q$  ( $\delta_{as}$ ) were observed in the Raman spectra instead of the expected two  $d$  and two  $t$ .

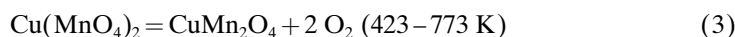
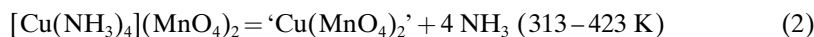
The appearance of IR-inactive Cu–N stretching modes in the IR spectrum of **1** shows the symmetry-lowering due to distortion of the regular square-planar  $\text{CuN}_4$  geometry. The splittings of  $\tilde{\nu}_s$ ,  $\delta_s$ , and  $\rho_1$  N–H bands or the  $\tilde{\nu}_{\text{as}}$  Cu–N band confirm the symmetry-lowering of the complex cation. The presence of this distorted cation structure together with shifts of N–H stretching bands show the presence of weak but well-defined H-bond(s) in **1** [7][10]. The unusual thermal behavior of **1** in the case of an N–H $\cdots$ O–Mn-centered redox reaction – instead of expected  $\text{NH}_3$  release – also confirms our results, pointing to the existence of a H-bond in **1**. Since the *Pauling* electronegativity is not suitable for the exact measurement of the electron density of the O-atoms in  $\text{MO}_4$  anions of transition metals with many electrons, the relative strength of this interaction cannot be determined based on the correlation between band position and electronegativity of the central atom in  $\text{MO}_4^{n-}$  anions.

*Thermal Decomposition of 1 in the Solid State.* The thermal-decomposition characteristics of **1** strongly depend on the presence of impurity **2** as well on the conditions of heating. On fast heating, or in the absence of a heat-conducting medium (e.g., alumina or an inert solvent such as  $\text{CCl}_4$ ), the decomposition reaction proceeds in one step like an explosion. The decomposition is of strongly exothermic character, starting with an explosion-like reaction at  $75^\circ$ . The gas-phase decomposition products are  $\text{NH}_3$ ,  $\text{O}_2$ , and oxidation products of  $\text{NH}_3$ , namely  $\text{N}_2$ ,  $\text{NO}$ ,  $\text{NO}_2$ , and  $\text{H}_2\text{O}$ . The presence of  $\text{N}_2\text{O}$  could not be detected. Nitrogen oxides and  $\text{N}_2$  may be formed from direct oxidation of  $\text{NH}_3$ . The primary oxidation products, however, could not be detected, since  $\text{NO}_2$  may form from the oxidation of  $\text{NO}$  due to the presence of  $\text{O}_2$ , or  $\text{NO}$  may also form from the decomposition of  $\text{NO}_2$ . The reaction of  $\text{NH}_3$  and nitrogen oxides may also lead to the formation of  $\text{H}_2\text{O}$  and  $\text{N}_2$ .

The solid residue contains  $\text{MnO}$  and  $\text{Mn}_3\text{O}_4$  as manganese-containing, and  $\text{Cu}$  and  $\text{Cu}_2\text{O}$  as copper-containing species. The heat of reaction is very high (308.6 kJ/mol). The ignition of **1** in an  $\text{O}_2$  atmosphere leads to the formation of metallic  $\text{Cu}$  and  $\text{Mn}_3\text{O}_4$  and to the formation of  $\text{H}_2\text{O}$ , a small amount of  $\text{NH}_3$ , and  $\text{N}_2$  as gaseous products. The ignition heat released is 635 kJ/mol, and **1** ignites with explosion under 8 bar of  $\text{O}_2$  pressure [4]. Compression of the crystalline structure under pressure causes a decrease in the N–H $\cdots$ O–Mn bond lengths, and the reaction heat of a subsequent redox reaction initiates further decomposition processes. Since the pressure was created by  $\text{O}_2$  gas, the reaction heat was higher during this process than the heat of thermal decomposition due to an almost complete oxidation of the  $\text{NH}_3$  present.

The analogous tetraamminecopper(2+) bis(perchlorate) decomposes by a rapid explosion without any possibility of isolating the intermediates or the end products [11][12]. Ignition properties were similar to those of the permanganate salt [4].

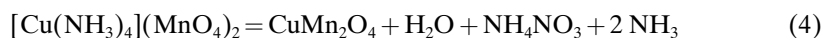
Preliminary thermogravimetric studies of the slow decomposition of **1** have already been performed [5]. According to the evaluation of weight-loss data, the decomposition mechanism was summarized by *Eqns. 2 and 3*. The intermediate phase was found to be an amorphous mass, while the final product was crystalline  $\text{CuMn}_2\text{O}_4$  [5].



Since the preparation of  $\text{Cu}(\text{MnO}_4)_2$  could not be performed by thermal dehydration of hydrated copper(II) permanganate [13], we tried to freeze the decomposition reaction at the stage of copper(II) permanganate formation. While our attempts aimed at the preparation of the compound failed, the presence of N-compounds and the absence of  $\text{MnO}_4^-$  ion could be observed in the solid residue.

To avoid fast decomposition and, thus, exclude explosive heat-induced degradation, a heat-convecting medium (alumina or an inert chlorinated solvent) was used during the study of the thermolytic reactions of **1**. In this case, the decomposition process of **1** could be followed. The thermal decomposition of **1** in the presence of 95% alumina was studied with simultaneous TG (thermogravimetry), DTG (differential thermogravimetry), DTA (differential thermal analysis), and evolved-gas detection ( $\text{NH}_3$ ) as well as with the monitoring of  $\text{H}_2\text{O}$  liberation. In the first step, 2 mol of  $\text{NH}_3$  as well as 1 mol of  $\text{H}_2\text{O}$  were released simultaneously in an exothermic reaction. The formation of these compounds was also confirmed by TG-MS results (Fig. 2). The IR spectra of the solid decomposition intermediate of **1** after the first step showed the presence of  $\text{NH}_4^+$  ion and  $\text{NO}_3^-$  ion, and the total absence of the  $\text{MnO}_4^-$  ion. The strong shift of the Mn–O stretching bands to the lower-wavenumber region in the IR spectrum of the decomposition intermediate shows a decrease in the oxidation number of manganese [14]. Since no  $\text{O}_2$  evolution was observed, the formation of  $\text{H}_2\text{O}$  must be the result of an unprecedented intramolecular redox reaction in solid **1**. To the best of our knowledge, **1** is the first permanganate salt known to decompose without  $\text{O}_2$  evolution during thermal treatment.

The first decomposition step of tetraamminecopper(2+) sulfate with the release of  $\text{NH}_3$  (2 mol) and  $\text{H}_2\text{O}$  (1 mol) is an endothermic process (199.8 kJ/mol) without any redox reaction. Since thermal deammoniation of the tetraamminecopper(2+) cation starts at  $75^\circ$  in the case of the sulfate salt, and the redox reaction starts at ca.  $65^\circ$ , **1** cannot be deammoniated by heating. The presence of the N–H $\cdots$ O–Mn linkage and the high oxidation ability of the  $\text{MnO}_4^-$  ion induce an intramolecular redox reaction with formation of  $\text{NH}_4\text{NO}_3$  instead of simple thermal deammoniation. Similarly, the thermal-decomposition temperature of the  $\text{MnO}_4^-$  ion is higher (above  $97^\circ$  [13][15]) than the temperature of the redox reaction. Therefore, the thermal decomposition of the  $\text{MnO}_4^-$  ion with the formation of  $\text{MnO}_2$  and  $\text{O}_2$  does not take place. Since only one of the  $\text{NH}_3$  ligands is oxidized, and the other forms a cation to neutralize the  $\text{HNO}_3$  formed, 2 mol of  $\text{NH}_3$  and 1 mol of  $\text{H}_2\text{O}$  are released into the gas phase. By lowering the oxidation state of manganese, the oxidizing ability of manganese-containing anions also decreases. Thus, the last 2 mol of  $\text{NH}_3$  are not oxidized in Mn-containing species at this low temperature. The oxidation of gaseous  $\text{NH}_3$  after thermal decomposition can be excluded, since  $\text{NH}_4\text{NO}_3$  is formed in the solid phase, and the temperature of the redox reaction is lower than the temperature of  $\text{NH}_3$  liberation from the tetraamminecopper(2+) cation. The equation of the slow thermal decomposition of **1** can be described by Eqn. 4.



The sum of the exothermic-reaction heat of  $\text{NH}_4\text{NO}_3$  formation (by the oxidation of  $\text{NH}_3$ ) and the endothermic release of  $\text{NH}_3$  gives an overall process of exothermic

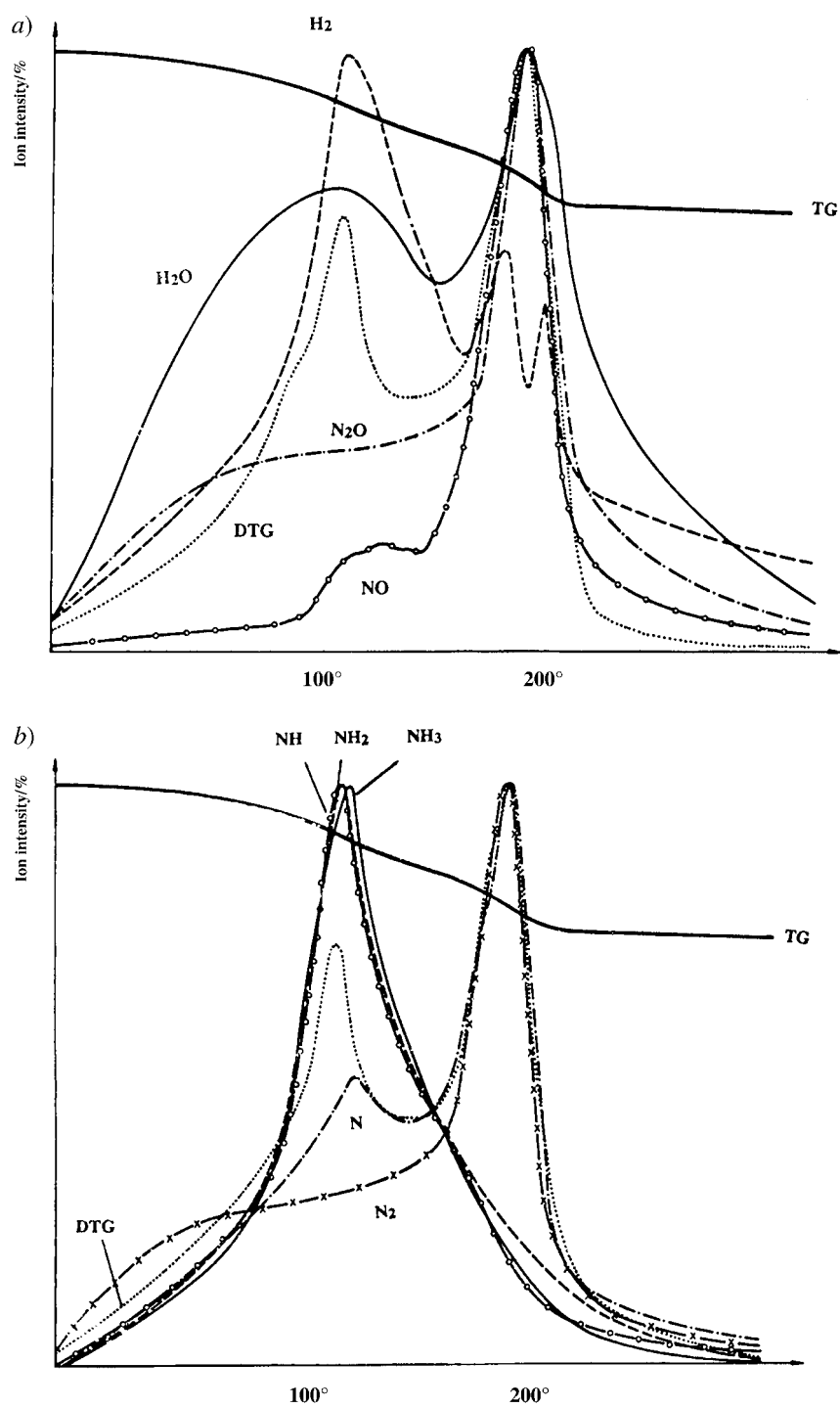


Fig. 2. TG-MS of 1 in alumina matrix



nature. In each step of the decomposition, the heat of reaction depends on the relative amounts of intermediates and contaminants formed during decomposition or aging (the ratio of these compounds may be affected by the heating rate, the presence of impurities, the age of the sample and the moisture content of the starting complex **1**). The effects of these factors can be clearly seen in the DSC (differential scanning calorimetry) spectra of fresh and 2-week-old samples of **1** (Fig. 3).

The solid decomposition intermediates are almost X-ray-amorphous powders, having highly diffuse, broad bands. The relatively small number of peaks show a simple (probably cubic) lattice. The stoichiometry of the residue gives the formula  $\text{CuMn}_2\text{O}_4$ . Since the Cu-containing solid residue does not dissolve in conc.  $\text{HNO}_3$  solution, the presence of CuO ( $\text{CuO/Mn}_2\text{O}_3$  mixture) may be excluded. However, a metallic Cu-containing residue may form as part of a fast decomposition, as evidenced by the formation of  $\text{Cu}(\text{NO}_3)_2$  with noxious gas evolution when the residue is treated with conc.  $\text{HNO}_3$  solution.

The second decomposition step gives, depending on the age of the sample, a weak exothermic or endothermic peak in the DSC curve, accompanied by the liberation of a small amount of gas ( $\text{NH}_3$  and its oxidation products). The gases formed are identical to the decomposition products of **2** [16]. The heat of reaction of the second step ( $110\text{--}160^\circ$ ) depends on the heat of reaction of the first step. In the case of a fresh sample, the heat of reaction of the first step is 289.8 kJ/mol, and the second decomposition step shows endothermic character (8.97 kJ/mol). In the case of aged samples (stored for 1 and 2 weeks in a refrigerator), the heat of reaction in the first step of decomposition is only 154.8 and 109.42 kJ/mol, respectively. There is no observable heat evolution/absorption in the case of the sample stored for 1 week. Some 50.3 kJ/mol heat is released in the second step in the case of the sample stored for 2 weeks. This step is probably a complex step of decomposition of the contaminant  $\text{NH}_4\text{MnO}_4$  (**2**) formed during the aging of the sample (exothermic), overlapped with endothermic phase transitions of  $\text{NH}_4\text{NO}_3$  formed in the first decomposition step [17].

The third decomposition step is an exothermic one at  $170\text{--}210^\circ$ . The heat of reaction depends on the age (and composition) of the sample (46.1–75.5 kJ/mol). Decomposition proceeds with evolution of  $\text{N}_2\text{O}$  and  $\text{H}_2\text{O}$  but without the release of  $\text{NH}_3$ ;  $\text{O}_2$  evolution is also not observed.

The third decomposition step is successfully frozen by quick cooling of the sample. The IR spectrum of the solid decomposition intermediates shows an unusual sharp peak at  $2200\text{ cm}^{-1}$ . This band is characteristic of gaseous  $\text{N}_2\text{O}$ . The existence of  $\text{N}_2\text{O}$ -gas inclusion in the solid residue shows that  $\text{N}_2\text{O}$  is formed in the solid phase and not from the oxidation of a gaseous N-compound. IR Bands characteristic of oxides of lower-valence manganese,  $\text{NH}_4^+$  ion, and  $\text{NO}_3^-$  ion are also observed. Based on the above results, the third decomposition step is identified as a noncatalysed and a metal-oxide catalysed thermal decomposition of ammonium nitrate with formation of  $\text{N}_2\text{O}$  and  $\text{H}_2\text{O}$  (see Eqn. 5). NO Formation as a side reaction during the thermal decomposition of  $\text{NH}_4\text{NO}_3$  is well-known [17]; NO may also be formed by fragmentation/decomposition of  $\text{N}_2\text{O}$  during MS measurements. Two  $\text{N}_2\text{O}$ -formation steps can be observed at this stage of decomposition. The first step probably originates from catalytic decomposition at a lower temperature, while the second one is probably a noncatalytic decomposition step (Fig. 2). Similar catalytic effects were observed in the thermal decomposition of

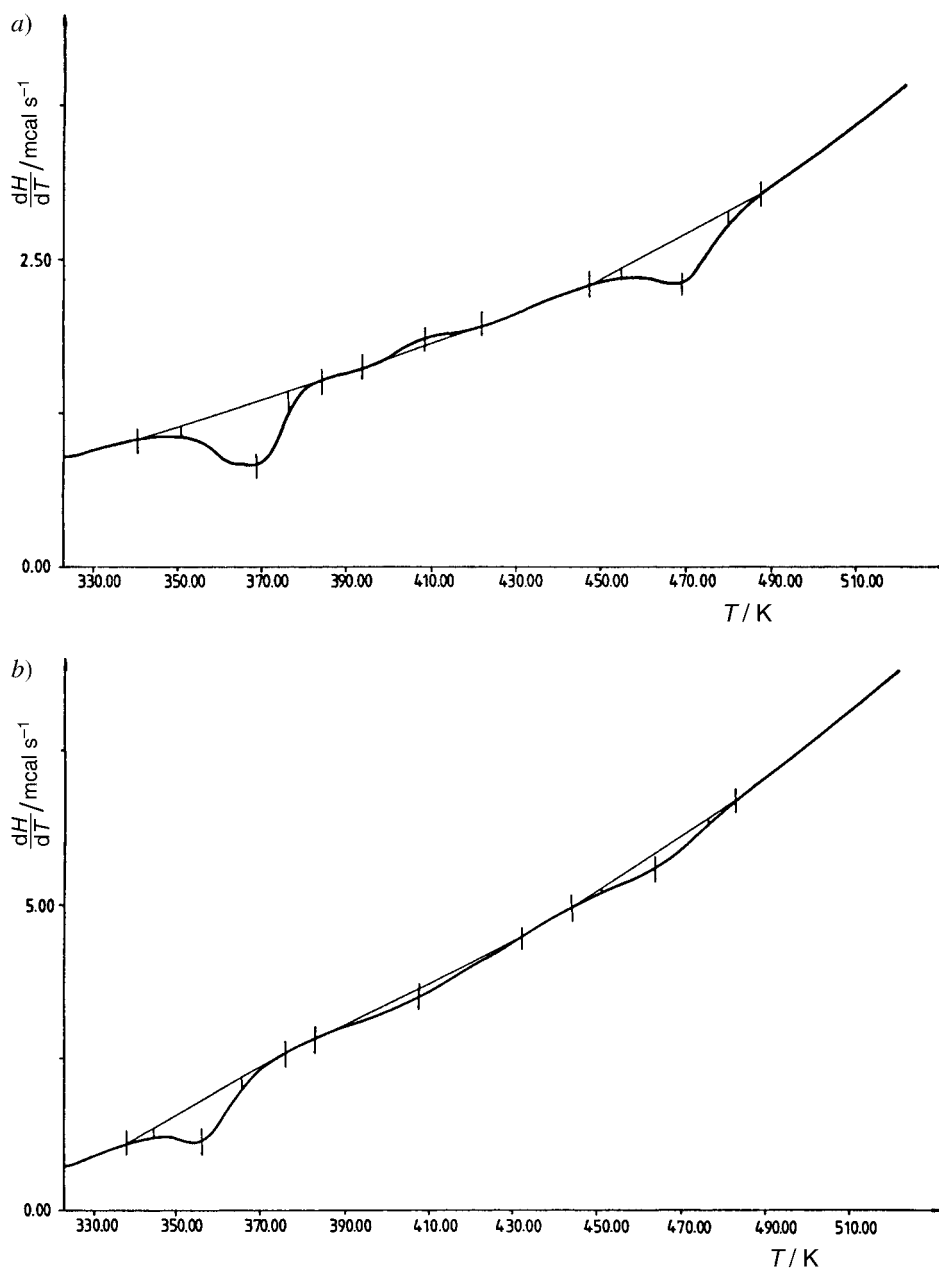


Fig. 3. DSC Curves of a) freshly prepared and b) aged samples of **1**

$\text{NH}_4\text{NO}_3$  [18]. Since the amount of  $\text{N}_2\text{O}$  is lower in the second decomposition step, we cannot exclude the possibility that this second step is the release of  $\text{N}_2\text{O}$  gas included in the solid decomposition intermediate.



*Low-Temperature Synthesis of Nanocrystalline  $\text{CuMn}_2\text{O}_4$  Catalyst Precursors.* Since the peak temperature of the first decomposition step of **1** is  $78^\circ$ , we used  $\text{CCl}_4$  (b.p.  $76.8^\circ$ ) instead of solid alumina as a heat-convecting medium. The suspension of **1** in  $\text{CCl}_4$  was refluxed for 1 h. During this time, **1** totally decomposed, and  $\text{NH}_4\text{NO}_3$  as well as a compound with a lower-oxidation-state Mn–O bond were detected in the solid residue by IR spectroscopy.

In addition to copper manganate, some copper manganese oxides also have manganese oxidation states lower than VII (e.g.,  $\text{Cu}_3(\text{MnO}_4)_2$ ,  $\text{CuMnO}_2$ , and  $\text{CuMn}_2\text{O}_4$  [19]). The formation of  $\text{CuMn}_2\text{O}_4$  from different manganese oxide and copper(II) oxide precursors is well-known. The temperatures of the syntheses were  $400\text{--}500^\circ$  [19], higher than the formation temperature of crystalline  $\text{CuMn}_2\text{O}_4$  in the thermal-decomposition process of **1** [5]. This is also confirmed by the lack of  $\text{CuO}$  and  $\text{Mn}_2\text{O}_3$  as primary decomposition products during the thermal decomposition of **1**.

Since the temperature of the intramolecular redox reaction in solid **1** is lower than the breakdown temperature of  $\text{MnO}_4^-$  ion (which is above  $97^\circ$  [12][15][16]), the Cu–O–Mn linkage of **1** remained without formation of  $\text{MnO}_2$ . This linkage serves as a basis for the evolution of a  $\text{CuMn}_2\text{O}_4$  spinel structure. Since copper is present in homogeneous distribution at a ionic level, and no diffusion mixing is required for the formation of a double-oxide structure, the evolution of a crystalline spinel structure starts at the temperature of  $\text{CuMn}_2\text{O}_4$  formation (ca.  $80^\circ$ ). Crystallization must be completed at higher temperatures (ca.  $230^\circ$ ). The only by-product of  $\text{CuMn}_2\text{O}_4$  formation was  $\text{NH}_4\text{NO}_3$ , which was removed from the decomposition product by washing with  $\text{H}_2\text{O}$ . With the use of  $\text{CCl}_4$  as a heat-convecting medium, the thermal decomposition of **1**, followed by washing of the solid residue with  $\text{H}_2\text{O}$ , gave a noncrystalline  $\text{CuMn}_2\text{O}_4$  catalyst precursor. This noncrystalline residue could be heated to induce crystallization. On heating this compound to  $200^\circ$  for 2 h, a slightly crystallized  $\text{CuMn}_2\text{O}_4$  spinel was obtained. The full profile fit of the X-ray diffraction data for the  $\text{CuMn}_2\text{O}_4$  phase shows a crystalline size of ca. 2 nm. Based on SEM (scanning electron microscopy) studies, these crystallites are located in a 100–300-nm amorphous matrix. At  $500^\circ$ , however, a totally crystalline  $\text{CuMn}_2\text{O}_4$  spinel could be prepared [5]. Elucidation of the mechanism of thermal decomposition of **1** revealed that the formation of  $\text{CuMn}_2\text{O}_4$  took place in the first decomposition step between  $60$  and  $80^\circ$ , and not by thermal decomposition of the  $\text{Cu}(\text{MnO}_4)_2$  intermediate at higher temperatures. This observation and the  $\text{H}_2\text{O}$  solubility of  $\text{NH}_4\text{NO}_3$  offer a simple, convenient method for the synthesis of noncrystalline  $\text{CuMn}_2\text{O}_4$  catalyst precursors at low temperature. Controlled heat treatment of noncrystalline  $\text{CuMn}_2\text{O}_4$  leads to controlled-size crystallites in the nm range.

We wish to express our thanks to Dr. *Attila Sebestyén*, *Margit Kovács-Toplak*, and *Katalin Papp* for their help in the experimental work.

## REFERENCES

- [1] H. G. Lintz, K. Wittstock, *Catal. Today* **1996**, 29, 457; A. F. Restovic, J. L. Gautier, *J. Braz. Chem. Soc.* **1994**, 5, 223; Baolian Zheng, Xiaolong He, Xingguo Yan, Zhongquan Wang, *Xiamen Daxue Xuebao, Ziran Kexueban* **1995**, 34, 214; P. A. Wright, S. Natarajan, J. M. Thomas, P. L. Gai Boyes, *Chem. Mater.* **1992**, 4, 1053; P. Porta, G. Moretti, M. Musicanti, A. Nardella, *Solid State Ionics* **1993**, 63-65, 257.
- [2] T. Klobb, *Compt. Rend.* **1886**, 103, 384; *Bull. Soc. Chim. Fr. [3]* **1890**, 3, 508.
- [3] A. Müller, I. Bösch, E. J. Baran, P. J. Aymonino, *Monatsh. Chem.* **1973**, 104, 836.
- [4] V. V. Gorbunov, L. F. Shmagin, *Fiz. Goreniya i Vzryva* **1972**, 8, 523.
- [5] N. Seferiadis, E. Dubler, H. R. Oswald, *Acta Crystallogr. Sect. C.* **1986**, 42, 942.
- [6] L. Kótai, K. Szentmihályi, T. Horváth, Á. Keszler, *Transition Met. Chem.* **2000**, 25, 293.
- [7] A. Novak, 'Hydrogen-Bonding in Solids', in 'Structure and Bonding', Springer-Verlag, Heidelberg, 1974, Vol. 18, p. 177; A. Lautie, F. Fromen, A. Novak, *Spectrosc. Lett.* **1976**, 9, 289; S. D. Hammann, *Aust. J. Chem.* **1978**, 31, 11; A. Rabold, R. Bauer, G. Zundel, *J. Phys. Chem.* **1995**, 99, 1889.
- [8] B. N. Cyvin, S. J. Cyvin, K. H. Schmidt, W. Wiegeler, A. Müller, *J. Mol. Struct.* **1976**, 30, 315; R. Acevedo, G. Diaz, *Spectrosc. Lett.* **1986**, 19, 563; A. Müller, B. Krebs, *J. Mol. Spectrosc.* **1967**, 24, 180; A. Krebs, A. Müller, A. Fadini, *J. Mol. Spectrosc.* **1967**, 24, 198; K. H. Schmidt, A. Müller, *J. Mol. Struct.* **1974**, 22, 343.
- [9] L. Kótai, Gy. Argay, S. Holly, K. Szentmihályi, Á. Keszler, B. Pukánszky, *Z. Anorg. Allg. Chem.* **2001**, 627, 114.
- [10] A. Müller, I. Boesch, E. J. Baran, P. J. Aymonino, *Monatsh. Chem.* **1973**, 104, 836; M. Trpkovska, B. Soptrajanov, *J. Mol. Struct.* **1997**, 408/409, 345.
- [11] U. C. Patil, V. R. P. Vernecker, *Thermochim. Acta* **1976**, 15, 257.
- [12] V. P. Guk, S. V. Savkina, V. A. Koroban, B. S. Svetlov, *Khim. Fiz.* **1990**, 9, 1670.
- [13] A. K. Galwey, S. A. A. Fakiha, K. M. Abd El-Salaam, *Thermochim. Acta* **1994**, 239, 225.
- [14] A. H. Jubert, E. L. Varetti, *J. Mol. Struct.* **1982**, 79, 285.
- [15] A. K. Galwey, S. A. A. Fakiha, K. M. Abd El-Salaam, *Thermochim. Acta* **1992**, 206, 297; M. E. Brown, A. K. Galwey, M. A. Mohamed, H. Tanaka, *Thermochim. Acta* **1994**, 235, 255; A. K. Galwey, S. A. A. Mansour, *Thermochim. Acta* **1993**, 228, 379; A. Feltz, F. Lindner, *Z. Anorg. Allg. Chem.* **1991**, 605, 117.
- [16] L. Kótai, P. Szabó, Á. Keszler, *Thermochim. Acta* **1999**, 338, 129.
- [17] M. E. E. Harju, J. Valkonen, *J. Therm. Anal.* **1993**, 39, 681; Bangning Wang, *Huaxue Xuebao* **1982**, 40, 1001; A. A. Shidlovskii, *Zh. Fiz. Khim.* **1965**, 39, 2163.
- [18] H. F. Johnstone, E. T. Houvouras, W. R. Schowalter, *Ind. Eng. Chem.* **1954**, 46, 702.
- [19] G. Rienaecker, K. Werner, *Z. Anorg. Allg. Chem.* **1964**, 327, 275; G. Rienaecker, K. Werner, *Z. Anorg. Allg. Chem.* **1964**, 327, 281.

Received February 27, 2002